

OPTIMIZATION OF FRESHWATER INFLOWS TO LAVACA-TRES PALACIOS, TEXAS, ESTUARY

By Yixing Bao,¹ Associate Member, ASCE, and
Larry W. Mays,² Member, ASCE

ABSTRACT: The companion paper by the writers developed a model for the determination of optimal freshwater inflows into bays and estuaries for the purpose of balancing freshwater demands with the various types of fish harvests. This model has been applied to determine the freshwater inflow needs into the Lavaca-Tres Palacios Estuary in Texas for various scenarios. The results of the model application are analyzed for various management alternatives, treatment of salinity constraints, and the desired levels of certainty for harvest regression equations. The comparison of the application results with previous models further illustrates the advancement of this new model. The new methodology can provide a powerful tool for analysis of "what if" type scenarios for decision makers to quantitatively analyze various water resources management strategies.

DESCRIPTION OF SYSTEMS

The computer model OPTFLOW (derived from optimal-flow estuarine model) developed by Bao (1992) and discussed in Bao and Mays (1994) for determination of the optimal freshwater inflows into bays and estuaries is applied to the Lavaca-Tres Palacios Estuary in Texas. This model interfaces the hydrodynamic-salinity transport model (HYD-SAL) with the nonlinear optimizer (GRG2). The constraints (see Bao and Mays 1993) for this optimization model include flow-fish harvest relationships, which are chance-constrained formulations; flow-salinity relationship, which is solved implicitly by a hydrodynamic transport model (HYD-SAL); and upstream flow requirements (monthly, seasonal, and annual flow limitations), marsh inundation requirements, and salinity bounds.

The Lavaca-Tres Palacios estuary (Fig. 1) covers an area of approximately 910 km² (350 sq m) and consists of eight smaller bays, namely, Matagorda Bay, Lavaca Bay, Keller Bay, Cox Bay, Carancahua Bay, Tres Palacios Bay, Turtle Bay, and Chocolate Bay. Similar to other Texas bay systems, this estuary is a shallow water estuary with water depths less than 4 m (13 ft), except in the Matagorda Ship Channel, which has depths of 12.2 m (40 ft). Most of the freshwater inflows reach the bay systems through the rivers and creeks, including gauged river flows; ungauged drainage area contribution to flow through creeks; and municipal, industrial, and agricultural return flows. The major rivers are the Colorado River located at the eastern segment of Matagorda Bay and Lavaca and the Navidad rivers located at the upper Lavaca Bay. For this bay system, tidal excitation and gulf inflow occur through Pass Cavallo, Saluria Bayou, Big Bayou, the Matagorda Ship Channel Gulf Pass, Parkers Cut, and Intercoastal Waterway (ICWW) ("Mathematical" 1979; "Lavaca" 1980).

¹Hydro., Texas Water Development Board, P.O. Box 13231, Austin, TX 78711-3231.

²Chair and Prof., Dept. of Civ. Engrg., Arizona State Univ., Tempe, AZ 85287.

Note. Discussion open until September 1, 1994. Separate discussions should be submitted for the individual papers in this symposium. To extend the closing date one month, a written request must be filed with the ASCE Manager of Journals. The manuscript for this paper was submitted for review and possible publication on December 22, 1992. This paper is part of the *Journal of Water Resources Planning and Management*, Vol. 120, No. 2, March/April, 1994. ©ASCE, ISSN 0733-9496/94/0002-0218/\$2.00 + \$.25 per page. Paper No. 5310.

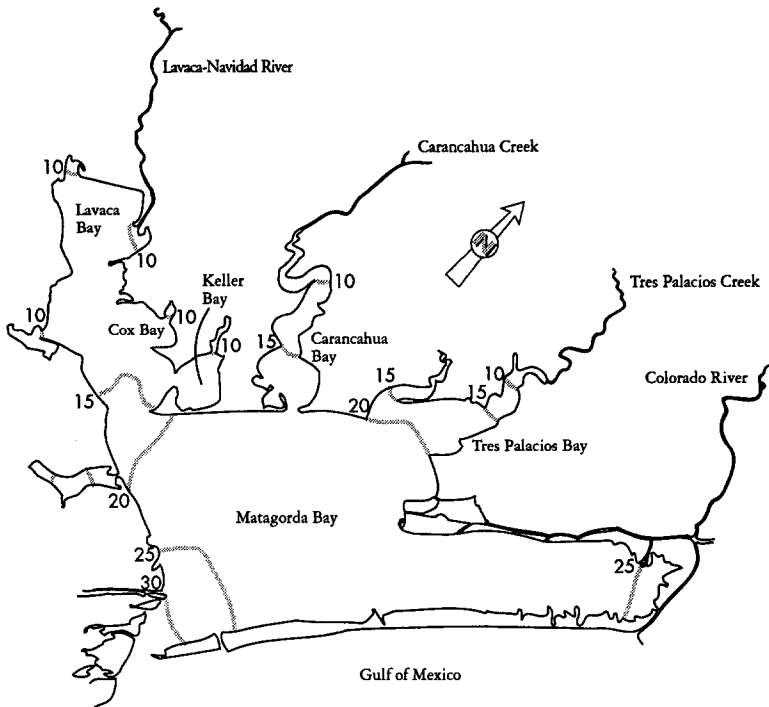


FIG. 1. Bay System Map and Example of Simulated Salinity Contours (ppt) in Lavaca-Tres Palacios Estuary

Mean annual precipitation directly on the $1,013 \text{ km}^2$ (250,485 acre) surface area is $1.065 \cdot 10^9 \text{ m}^3$ (864,000 acre-ft/yr) or 1.05 m/yr (41.4 in./yr). The evaporation loss is estimated from pan evaporation data as $1.44 \cdot 10^9 \text{ m}^3/\text{yr}$ (1,171,000 acre-ft/yr) over $1,013.7 \text{ km}^2$ (250,485 acres) water surface area, which is equivalent to 1.36 m/yr (53.5 in./yr).

There are three types of tidal information available for the Matagorda Bay system: (1) Tidal records (most accurate but incomplete), (2) simulated (harmonic) records; and (3) regression relationships that relate to bay tidal station records. The combination of these three and the simulated tides for 1984 were used. The entire tidal data for a year were separated for each month and tested for use of: (1) Entire month of tides; (2) one tidal cycle (25 h) averaged over a month period; and (3) two tidal cycles (50 h) averaged over a month. The two tidal cycle data were used in this application. The use of an entire month tidal data is computationally expensive and too data specific (for the conditions in that year only), while only a one-day (tidal cycle) application was found to be insufficient from the preliminary runs of HYD-SAL. The two-day tidal cycle data are presented in Fig. 2.

Salinity viability limits for Texas bays and estuaries have been established to account for spatial distribution (e.g., from the upper estuary to the middle estuary and to the lagoonal arm of the estuary) and time variation (on a monthly basis). Factors considered to determine the salinity viability limits are successful reproduction, percent survival, percent fertilization, metabolic rates, and catch ratio versus salinity tolerance in target species ("Lavaca" 1980). Salinity patterns were studied based on the salinity simulation

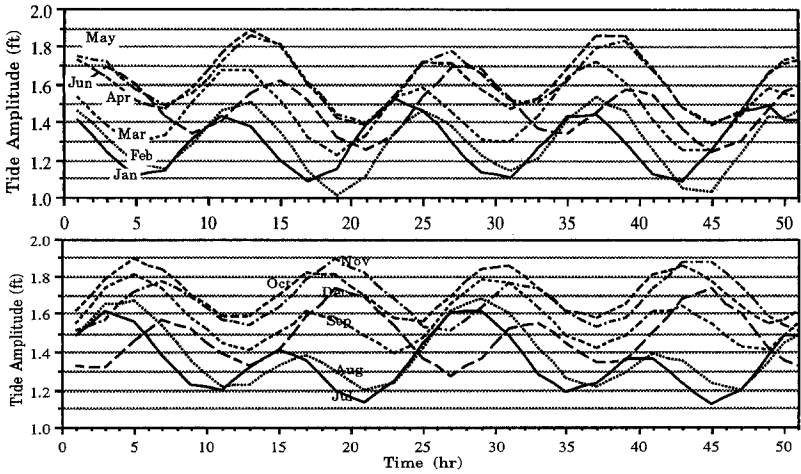


FIG. 2. Monthly Averaged Tidal Cycles for Lavaca-Tres Palacios Estuary from 1984 Tide Data (25 hrs/cycle, 2-day) (1 ft = 0.3048 m)

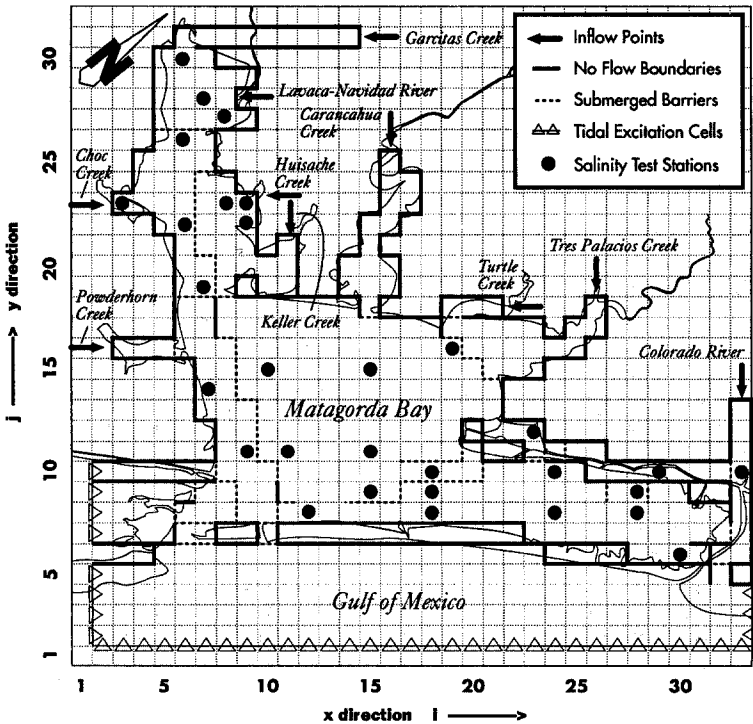


FIG. 3. Computation Grid for Lavaca-Tres Palacios Estuary

results of applying HYD-SAL and the actual salinity measurement data. The 30 salinity test (control) stations established to represent the spatial salinity distribution over the bay system are indicated by the solid dots in Fig. 3. Since the averaged monthly salinity at each grid is computed and stored in the model, the actual number of salinity constraints is 360 for the 30 stations. The salinity bounds used in this work are the same as those presented by Tung et al. (1990).

The major sources of freshwater inflow into the bay system are: (1) Gauged river flow; (2) ungauged flows; and (3) direct precipitation on the estuarine surface area. Since the salinity is affected by the total amount of freshwater into the bay system, the total freshwater inflow needs to be considered in the estuarine management model. However, among these three freshwater sources, the gauged river flow is the most important one because of its magnitude and the only one that can be regulated for the estuarine management. The ungauged flows have been estimated by separate models, which are not as accurate as the recorded historical river flows.

In theory, all three freshwater sources can be treated as decision variables in the optimization model. The optimal precipitation and the runoff, however are beyond human control. Therefore, the issue is not the ungauged flow and precipitation to be chosen as decision variables but how accurate should be the estimation of these flows. The ungauged flow can be estimated (or predicted) and then considered as constant in the optimization model. Another way is to consider the total flow as a decision variable, but relate the ungauged flows to the major river flow by a regression model or simply by a gauged/ungauged flow ratio. Once the optimum is reached, the optimal total flow can then be partitioned into river flow requirement (gauged) and the portion of creek flow (ungauged).

In the present paper, the estuarine model application does not focus on real-time management on a daily or weekly basis, but rather is used as a long-term planning assessment tool (e.g., on an annual basis). The monthly flows of major rivers, namely the Lavaca River and the Colorado River, are considered as decision variables, while the flow (runoff) of other creeks are treated as constant. The values of the constant flow in the smaller creeks, however, can be varied to investigate the sensitivity of runoff on the bay salinity if necessary.

The multiple regression equations for fish harvest were derived using the independent variables of Colorado River flow, Lavaca River flow, or a combination of both river flows (see Table 1). Five fish species were con-

TABLE 1. Modified Regression Equation Characteristics of Fishery Harvest and Freshwater Inflow Relations (Derived from Historical Gauged Flow and Commercial Harvest Records)

Index (1)	Species (2)	Equation (3)	Standard Error σ_k (4)	Freshwater inflow used in equation (5)
1	All shellfish	Eq. (1)	± 482.6	Lavaca delta
2	Spotted seatrout	Eq. (2)	± 0.290	Lavaca delta
3	Red drum	Eq. (3)	± 0.287	Colorado delta
4	All penaeid shrimp	Eq. (4)	± 463.3	Colorado delta
5	Blue crab	Eq. (5)	± 298.3	combined

sidered and seasonal flows were chosen as independent variables. The resulting equations follow:

For all shellfish

$$H_1 = 3,109.5 - 3.782QS_1 + 2.553QS_2 - 12.14QS_3 \dots\dots\dots (1)$$

For spotted seatrout

$$\ln(H_2) = 7.21 - 1.247 \ln(QS_1) + 1.153 \ln(QS_2) - 0.404 \ln(QS_4) \dots (2)$$

For red drum

$$\ln(H_3) = 4.134 + 0.697 \ln(QS_2) - 0.869 \ln(QS_3) \dots\dots\dots (3)$$

For all penaeid shrimp

$$H_4 = 1888.6 - 1.061QS_1 + 1.088QS_2 - 1.071QS_5 \dots\dots\dots (4)$$

For blue crab

$$H_5 = 289.5 + 1.725QS_3 + 0.429QS_4 + 0.202QS_5 \dots\dots\dots (5)$$

where H_k = commercial harvest of species $k \times 1,000/\text{lb}$ (1 lb = 0.45 kg); $QS_1, QS_2, QS_3, QS_4,$ and QS_5 = mean monthly freshwater inflow in acre-feet during the season January–March, April–June, July–August, September–October, and November–December, respectively (1 acre-ft = 1,233.5 m³).

APPLICATION

The OPTFLOW model application focused on four key issues: (1) To evaluate the impact of the approximation scheme for the reduced gradient and function evaluation on the problem solution; (2) to test the effect of the augmented Lagrangian (AL) parameters on the solution process (Bao and Mays 1994); (3) to compare the results with that of the Tung et al. (1990) model; and (4) to explore the global optimum issue.

Although an increase of time step will reduce the computer CPU time, the time step is limited due to the explicit formulation used in the hydrodynamic model (HYD). The time step in the hydrodynamic model, HYD, is controlled by considerations for stability, convergence and compatibility. For a given grid network, the maximum allowed time step is limited by the following criterion, so-called Courant condition, for a stable solution.

$$\Delta t \leq \frac{\Delta S}{\sqrt{2gd_{\max}}} \dots\dots\dots (6)$$

where Δt = time step; ΔS = grid size; and d_{\max} = maximum water depth in the bay system. For the Matagorda Bay system (Fig. 3), with a grid dimension of 1 nautical mile [1.85 km (6,076 ft)], maximum depth of 13.7 m (45 ft), the Courant number is about 1.9 min. For this reason, the time step of 1.5 min. is used for the hydrodynamic model. Theoretically, the salinity model (SAL) is unconditionally stable for any size of time step or spatial distance since it is formulated using an alternating direction implicit (ADI) scheme. The same grid network is used for SAL and time steps at 25 h (one tidal cycle), because the hydraulic inputs used in the transport model is net velocities over a tidal cycle.

The model results (i.e., total annual minimum freshwater inflow needs)

are affected by a number of factors such as the number of AL objective gradient approximations allowed (NDSOQ), initial conditions, inner optimizer GRG2 parameters, AL parameters, required harvest reliability P_h , and more importantly the salinity convergence factor S_c . When the model is run to evaluate a particular parameter such as P_h , efforts have been made to exclude the possible affecting factors by maintaining all other variables at the same level (condition). In cases for the uncontrollable important factors, such as the final convergence factor S_{cf} (or maximum salinity violation at the end of a program run) and the number of violated salinity constraints (that the magnitude of the salinity violation is less than the convergence factor S_c), some other parameters might be changed to adjust the situation accordingly based on the results of the analyses. All application runs of the model were performed on a Cray Y-MP8/864 computer system.

RESULTS AND COMMENTS

The results of various application runs are presented in Table 2 for different numbers of reduced gradient calls by the approximation technique (see Bao and Mays 1994). The second column of gradient calls by approximation (NDSOQ) is the number prespecified for the program run. For case 1, NDSOQ was set at 100, but the total gradient calls is only 31 so that it only took one outer loop iteration to update the reduced gradient matrix. When NDSOQ is 10 or less the impact of NDSOQ on the optimal annual total flow becomes negligible. The optimal annual total flow is higher for case 4; because the final convergence factor of salinity (S_{cf}) is significantly lower, which translates to more flow being required in the area near the Colorado delta to reduce the salinity violation out of the upper bounds. The number of total function calls (number of times the simulator is solved) in column 6 includes function calls for updating the objective function and the function calls required for computing the reduced gradient. The execution time requirement (CPU) for the model is directly proportional to the number of calls for estimation of the reduced gradient by hydrodynamic transport simulation (in column 4). Using the forward difference method, each call for computation of the reduced gradient by simulation (when $NDSOX \geq NDSOQ$) requires 36 simulation calls for simulating the monthly salinities (12 monthly simulations required for updating the objective and 24 simulations are required for computing the reduced gradient). The final salinity convergence value the model reaches is S_{cf} , which is equal to the maximum salinity violation for all salinity constraints (i.e., $S_{cf} = \max C_i, i = 1, 2, \dots, 360$).

AUGMENTED LAGRANGIAN PARAMETERS

The three parameters considered for the augmented Lagrangian algorithm (AL) are the initial augmented Lagrangian multiplier μ^0 , initial penalty σ^0 , and the penalty multiplier $\Delta\sigma$ (see Bao and Mays 1994). In Fletcher's (1975) algorithm, the recommended μ^0 , σ^0 , and $\Delta\sigma$ are 1.0, 10.0, and 10.0, respectively. The application runs of OPTFLOW for the penalty multiplier ($\Delta\sigma$) were designed to examine whether the program converges faster (with fewer outerloop iterations) for higher $\Delta\sigma$ values.

Results are summarized in Table 3. In Table 3(a), the number of gradient calls by approximation (NDSOQ) is set to a large number (500) so that the reduced gradient is only updated once at the beginning of a program run by calling the simulator, and all other reduced gradients are computed by

TABLE 2. Results of OPTFLOW for Different Number of Gradient Approximation by $\partial s/\partial Q$ (NDSDQ)

Case (1)	Gradient calls by $\partial s/\partial Q$ (NDSDQ) (2)	Optimal annual flow (1,000 acre-ft) (3)	Gradient calls by simulation (4)	Total gradient calls (5)	Total function calls (6)	S_c (7)	Total outerloop iteration (8)	S_{of} (9)	CPU (s) ^a (10)
1	100	1,967.292	1	31	267	0.2	4	0.193	444.0
2	10	1,890.455	3	29	373	0.2	5	0.143	1,328.5
3	5	1,889.961	6	26	451	0.2	5	0.183	2,657.5
4	3	1,906.646	5	13	343	0.2	6	0.087	2,216.6

^aOn Cray Y-MP8/864.

Note: 1 acre-ft = 1,233.5 m³; $\sigma^O = 10.0$; $\mu^O = 1.0$; and $\Delta\sigma = 10.0$.

TABLE 3. Results of OPTFLOW for Different Penalty Multiplier ($\Delta\sigma$) Used in Augmented Lagrangian Method

Case (1)	Penalty multiplier $\Delta\sigma$ (2)	Optimal annual flow (1,000 acre-ft) (3)	S_{cf} (4)	Total gradient calls (5)	Total function calls (6)	S_v (7)	Total outerloop iteration (8)	Violated salinity constraints (9)	CPU (s) (10)
(a) NDSOQ = 500.									
1	10	1,971.636	0.187	31	284	0.2	4	7	444.1
2	50	1,988.431	0.141	161	1,036	0.2	7	7	445.3
3	100	1,969.597	0.185	54	677	0.2	4	6	444.2
4	500	1,997.657	0.197	86	977	0.2	5	8	444.9
(b) NDSOQ = 10.									
1	10	1,890.455	0.143	29	373	0.2	5	5	1,328.5
2	50	1,905.524	0.100	39	570	0.2	5	3	1,770.8
3	100	1,906.341	0.074	48	703	0.2	5	3	2,212.1
4	500	1,923.657	0.013	41	619	0.2	5	3	2,211.9

Note: 1 acre-ft = 1,233.5 m³; $\sigma^0 = 10.0$; $\mu^0 = 1.0$, and $\Delta\sigma = 10.0$.

an approximation of $\partial s/\partial Q$ without simulator calls. The actual total number of approximations of $\partial s/\partial Q$ for $\partial F/\partial Q$ during a program run is in the range of 31 to 161. The total function calls, column 6 in Table 3 is the number of function calls for updating the objective function plus the function calls required for updating the reduced gradient of $\partial F/\partial Q$. To compute $\partial F/\partial Q$ using forward differences, 36 function calls are needed, while if the reduced gradient is approximated by $\partial s/\partial Q$, the required number of function calls is counted as one. In column (7), S_c is the prespecified salinity convergence factor (or criterion) for the AL loop and S_{c_f} in column 4 is the maximum salinity violation (or final convergence factor) at the end of the program run. The number in column 9 is the total number of salinity constraint violations (out of 360 salinity constraints) while the convergence criterion is satisfied.

The results presented in Table 3(b) are more accurate than those in Table 3(a) due to the smaller NDSOQ, which is paid by a much higher CPU time requirement. The smaller the NDSOQ used, the more hydrodynamic transport simulation calls are required to update the reduce gradient. Thus, higher CPU time is needed, since the computer execution time is directly proportional to the number of the hydrodynamic transport simulations required. In both cases, the results show that the higher $\Delta\sigma$ value does not necessarily reduce the number of outerloop iterations. The reason is that the higher penalty multiplier results in bigger changes in the optimal monthly flow solved by the inner optimizer between two outerloop iterations, which causes more frequent switches of salinity constraint violations. In other words, because of the big changes in optimal monthly flow from an outerloop iteration k to $k + 1$, some salinity constraints which are satisfied in iteration k will probably be violated in $k + 1$ outerloop iterations. This is illustrated in Figs. 4 and 5, which are excerpted from the results for case 2 in Table 3(a).

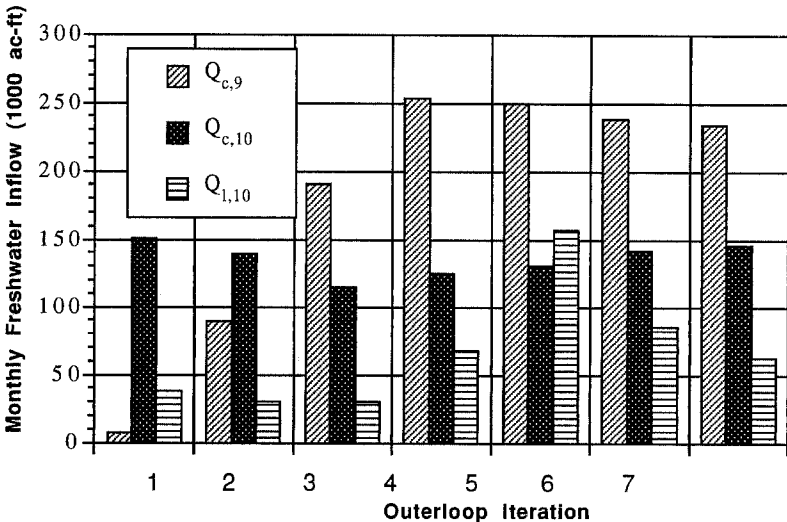


FIG. 4. Example of Optimal Monthly Freshwater Inflows at Each Outerloop Iteration Solved by Inner Optimizer ($Q_{c,9}$ = Flow from Colorado in September; $Q_{c,10}$ = Flow from Colorado in October; $Q_{l,10}$ = Flow from Lavaca in October) (1 acre-ft = 1,233.5 m³)

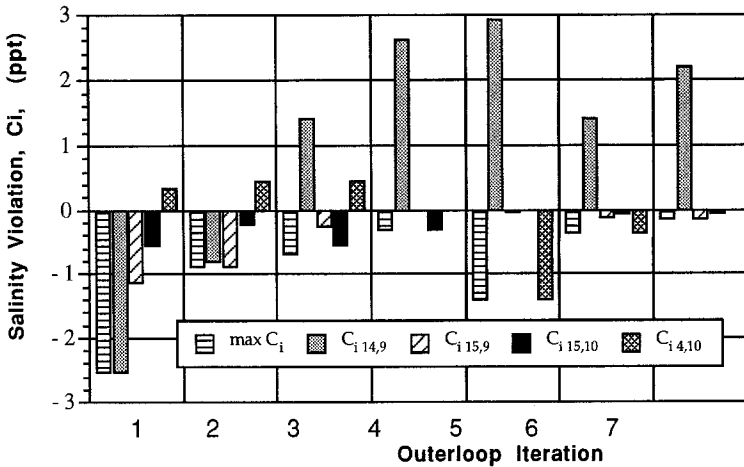


FIG. 5. Examples of Salinity Violation at Each Outerloop Iteration (Numbers in Subscripts Represent Test Station and Month, Respectively) ($\mu^o = 1, \sigma^o = 1.0$ and $\Delta\sigma = 50$, based on Case 2, Table 3)

Fig. 4 shows an example of change of the optimum of three decision variables for the inner problem between the outerloop iterations. The corresponding salinity violation for four of the salinity constraints is presented in Fig. 5. In addition, the maximum salinity violation among all 360 salinity constraints at each outerloop is plotted in Fig. 5 for comparison. The negative value of the violation term c_i indicates that the constraint is violated so that the salinity is either greater than the upper bound or lower than the lower bound, i.e., $c_i = \min[s_i - \bar{s}_i, \underline{s}_i - s_i]$.

At outerloop iteration 1, the maximum salinity violation occurred for constraint $c_{i14,9}$ (test station 14 near the Colorado Delta in September, see Fig. 5) due to the low optimal flow of $Q_{c,9}$ (Colorado River flow in September) determined by the inner optimizer for given initial augmented Lagrangian parameters (Fig. 4). In this case, the salinity at $c_{i14,9}$ is greater than the upper bound. From outerloop iterations 2 to 4, with increase of $Q_{c,9}$ (as well as changes in other decision variables), the salinity constraint is satisfied and the maximum salinity violation for all constraints (convergence factor, an absolute value) is also decreased significantly (Figs. 4 and 5). At outerloop iteration 5, the previously satisfied constraint $c_{i4,10}$ (at station 4 in Lavaca Bay in October) becomes violated because of the high flows, $Q_{i,10}$ (Lavaca River flow in October), $Q_{c,9}$, and $Q_{c,10}$. The convergence factor bounds back from 0.3 to 1.4, which requires two more AL iterations to reach final convergence.

HARVEST RELIABILITY REQUIREMENTS

Fig. 6 summarizes the comparison of using the models developed by Bao and Mays (1994), and by Tung et al. (1990). These models were considered to represent three different scenarios regarding the salinity constraints. In the Tung et al. (1990) model, the salinity regression equations are used to form the chance constraints. The results presented for reliability (curve A in Fig. 6) are under the conditions that the required reliability of the salinity constraints is set at 0.25 for the Upper Lavaca Bay (affected mainly by Lavaca River flow) and 0.4 for the eastern arm of Matagorda Bay (affected

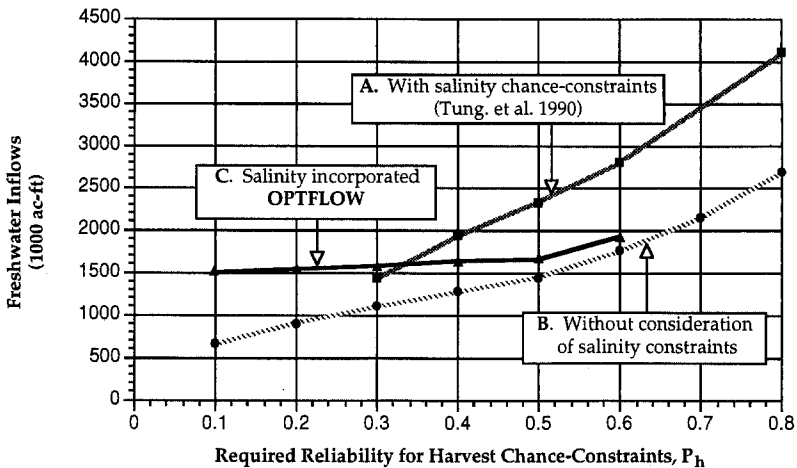


FIG. 6. Comparison of Optimal Annual Total Freshwater Inflows for Different Methods for Incorporating Salinity Constraints (1 acre-ft = 1,233.5 m³)

mainly by Colorado River flow). The results for curve *B* are with the salinity regressions removed from the constraint sets to examine the impact of the salinity constraints on the freshwater inflow. In the OPTFLOW, the spatial salinity pattern is simulated through the hydrodynamic transport model to account for temporal and spatial variability of salinity. The corresponding results are presented in curve *C*.

The resultant annual total optimal freshwater inflow from the OPTFLOW increases as the desired reliability of harvest chance constraints (P_h) increases, which is consistent with the findings in Tung et al. (1990). The difference in the freshwater inflow between the *B* and *C* curves is the amount of freshwater required to satisfy the 360 salinity constraints (test stations \times 12 months). The magnitude of the difference in freshwater inflow requirements decreases as P_h increases, since the increased amount of freshwater inflow with increase of P_h will also help reduce the salinity level in the bay system and satisfy more salinity conditions. Thus, with high reliabilities (P_h) for the harvest chance constraints, only a smaller amount of additional freshwater is required to satisfy the salinity constraints.

The maximum of the required reliability of fish harvest (P_h) that can be reached is about 0.65 for OPTFLOW as compared to the overall reachable reliability for *A* is only 0.1 or 0.43 depending on which set of salinity bounds is used. For *A*, the salinity-freshwater regression equations, derived for the entire estuary system do not describe the spatial distribution, which in part contributes to the uncertainty of the salinity regression equations (higher standard deviation and lower coefficient of determination). Hence, as the P_h increases the optimal freshwater inflow determined by the Tung et al. (1990) model is much higher than that computed by OPTFLOW.

SALINITY CONVERGENCE

The final optimization results are affected by many factors. One of the most important factors is the final salinity convergence factor, S_f which is equal to the absolute value of the maximum salinity violation at the salinity test stations. The change of salinity value is relatively insensitive as compared

to the magnitude of change of freshwater inflow due to the nature of the bay system (tidal sources and vast bay area). The ideal (or true optimal) solution is that no salinity constraints should be violated at any station during any time period (all months). This true optimum may not exist (infeasible problem), depending on how the salinity bounds are specified. There are two approaches to solve this problem: (1) To refine the salinity bounds; and (2) to set a salinity convergence criterion. If the maximum salinity violation is less than the criteria specified then the problem has converged and the optimal solution is reached.

Although the salinity constraints can be relaxed at the salinity test station to overcome the infeasibility problem, it is reasoned in the present study that for the real-world problem, it is more realistic to set the salinity convergence criteria as small constant(s) instead of zero. This salinity convergence criterion can be varied if necessary for sensitivity analyses or for providing alternatives for decision makers. In the present study, the salinity convergence criterion is set in the range from 0.2 to 0.5.

Fig. 7 shows an example of the intermediate results of maximum salinity violation and number of salinity constraints for each outerloop iteration (updating AL parameters). The initial convergence factor is set at a large

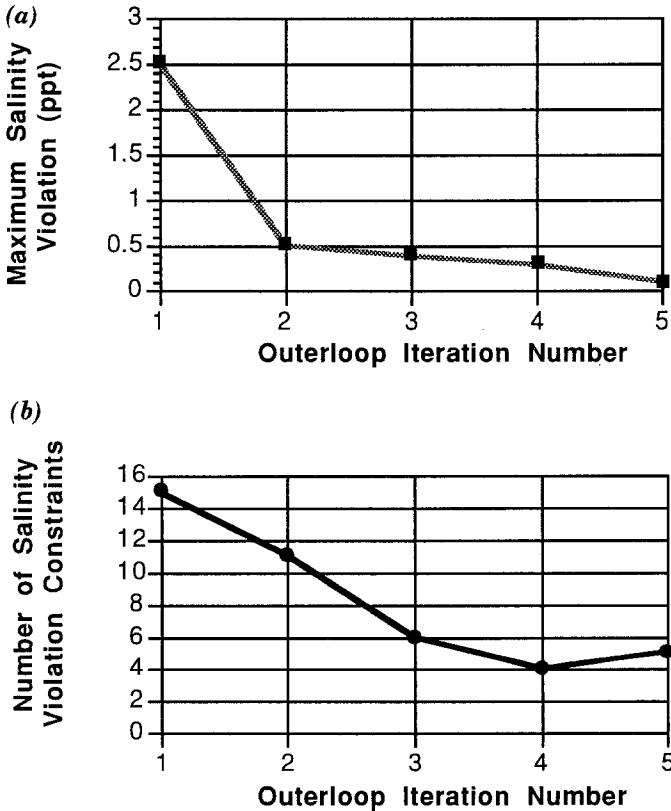


FIG. 7. Outerloop (AL) Iteration for OPTFLOW Model: (a) Salinity Convergence Factor; (b) Number of Salinity Constraints Violations (based on Case 4, Table 2)

number (50,000) and initial AL parameters of μ^o , σ^o , and $\Delta\sigma$ are set at 1.0, 10.0, and 10.0, respectively. The salinity convergence criterion is set at 0.2 and the final convergence factor reaches to 0.087. Although it is not shown in Fig. 7, the first AL iteration is the most efficient one to reduce both maximum salinity violation and the number of violated constraints. This is concluded by comparison of the intermediate results at the first AL iteration with those obtained by running the Tung et al. (1990) model (without salinity constraints) and then converting the optimal solution to an input file to run HYD-SAL for simulating the temporal and spatial salinity to examine the salinity violation situation. In general, both the convergence factor (or the maximum salinity violation) and the number of violated salinity constraints reduce dramatically at the first outerloop iteration (run with the initial AL parameters). As shown in Fig. 7, both the number of salinity constraint violations and the convergence factor reduce significantly in the first few AL iterations. In this example run, OPTFLOW converges at the fifth outerloop iteration. In general, OPTFLOW converges within three to seven AL iterations, with some exceptions (up to 13 iterations).

Optimal Monthly Flows

The optimal monthly freshwater inflows for the two major rivers in the bay system, namely the Colorado River and the Lavaca River for a particular run of the model is presented in Figs. 8 and 9 as examples. The required probability for fishery harvest constraints P_h is set at 0.1 and 0.6, respectively. In several months (e.g., January to March for the Lavaca River) the optimal monthly freshwater inflow is relatively low due to the low values of the lower bounds of the monthly freshwater inflow that are used in the model (extracted from the historical flow data records). In fact, when P_h is 0.1 (Fig. 8), the optimal flow for the Lavaca River for months from January to March are actually at the lower bounds. In reality, the decision maker

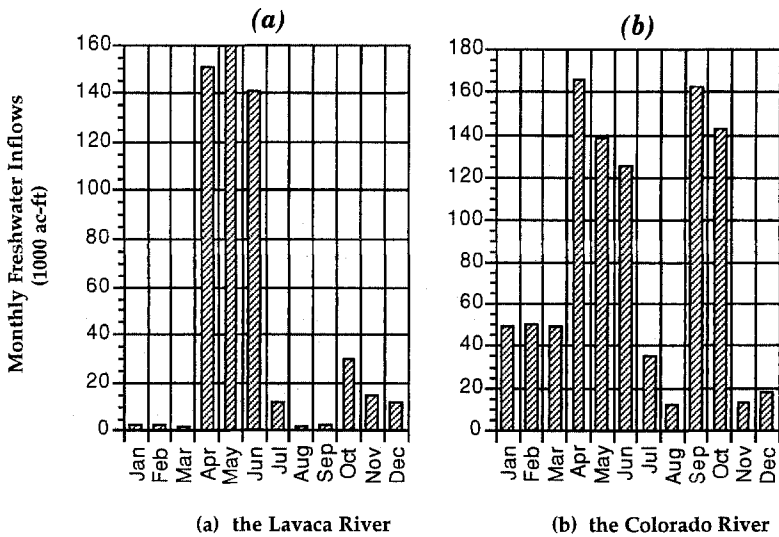


FIG. 8. Example of Optimal Monthly Freshwater Inflows for Major Rivers in Lavaca-Tres Palacios Estuary ($P_h = 0.1$): (a) Lavaca River; (b) Colorado River (1 acre-ft = 1,223.5 m³) ($S_{cf} = 0.265$ and AL iteration = 5)

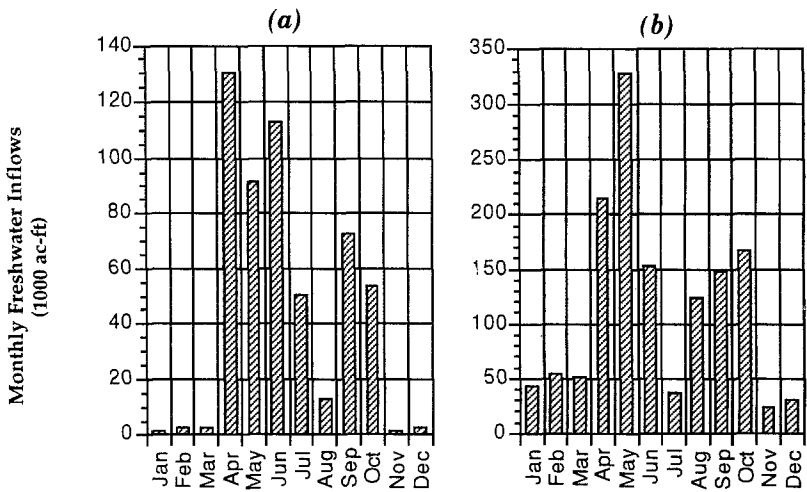


FIG. 9. Example of Optimal Monthly Freshwater Inflows for Major Rivers in Lavaca-Tres Palacios Estuary ($P_h = 0.6$): (a) Lavaca River; (b) Colorado River (1 acre-ft = 1,223.5 m³) ($S_{cf} = 0.087$ and AL (Outerloop) iteration = 5)

may want to increase the lower bound of the monthly freshwater inflow to consider the water demand of upstream users. The optimal monthly freshwater inflow for that river, therefore, will be changed accordingly. To be consistent the bounds on monthly or seasonal flow are not changed through the application runs.

As shown in Figs. 8 and 9, there are two peaks of the monthly flow requirements on an annual basis, namely April–June and September–October, which mimic the normal river flow pattern. This can be explained by the fact that most constraints, especially the marsh inundation and harvest constraints, require more freshwater for these periods. The coefficients of the seasonal variables QS_2 (April–June) and QS_4 (September–October) in the fish harvest regression equations are positive for most species, which force the high flow to satisfy the harvest constraints.

Spatial Variability of Salinity and River Flows

When the required reliability of the harvest chance constraints P_h increases from 0.1 to 0.6, the optimal annual flow for the Colorado River increases significantly, but the Lavaca River flow requirement remains at relatively the same level [$6,537 \cdot 10^8$ m³ (about 530,000 acre-ft) in Figs. 8 and 9]. This is different from the results using the Tung et al. (1990) model, in which the optimal annual flow for the Lavaca River increases significantly as P_h increases. The phenomenon of small changes in annual flow of the Lavaca River flow can be explained by the following factors.

The first factor is spatial variation of salinity. Within the estuary, salinity is normally low in the Lavaca Bay (upper estuary), and higher in the lagoonal arm of an estuary (or lower estuary) and in the middle estuary. With a low reliability P_h , the optimal flow will be low and the salinity in the entire bay system tends to be high if salinity constraints are not considered. In this case (low flow and high salinity), it is more efficient to reduce the salinity in the upper bays (i.e., the Lavaca Bay) by increasing the freshwater flow from the upper estuarine rivers (i.e., Lavaca River). Hence, even if the P_h

is low, because of the salinity constraints, the upper estuarine river (Lavaca River) is required to release relatively high flow to maintain the normally low salinity conditions in the upper bays. On the other hand, since the salinity in the upper bay is normally low, the upper estuarine river flow cannot be too high to have the salinities violate the lower bounds in the upper bays. Therefore when P_h is high, the additional flow required to satisfy the harvest chance constraints is mostly contributed from the lagoonal arm estuarine river (i.e., Colorado River).

The second factor is the difference in flow magnitude. The recorded flow magnitude of the Colorado River is more than twice the Lavaca River flow. In case of high P_h , naturally more flow will be provided from the Colorado River.

Briefly, the reason that the Tung et al. (1992) model cannot represent this phenomenon of small changes in the annual Lavaca River flow regardless of the change of P_h is that the salinity regression equations cannot account for the spatial variability of the salinity and oversimplifies the complicated hydrodynamic transport processes affecting the salinity such as tides, winds, evaporation, and precipitation.

Optimal Fish Harvest

As shown in (1), (2), and (4), respectively, shellfish, sea trout, and all shrimp have negative coefficients of the seasonal flow QS_1 (for the period from January to March), and all species except blue crab have a positive coefficient for the seasonal flow for April, May, and June (blue crab regression equation does not include this seasonal flow). Only two species of sea trout and blue crab have the seasonal flow from September to October as an independent variable in their regression equations. Although the sea trout regression equation has a negative coefficient for this seasonal flow, while the coefficient in the blue crab regression equation is positive, the chance constraint of sea trout is much easier to satisfy as compared with that of blue crab (Table 4). Therefore, the overall impact of the harvest constraints will tend to increase the monthly flows from September to October due to the positive seasonal coefficient in the blue crab regression equation.

Table 4 shows examples of expected fish harvest for the five species considered. The harvest target is set as the lower bound of the fish harvest for the particular species to be satisfied in the chance constraints. For purposes of illustration, the historical mean of the harvest for each species is used as the harvest target. The expected harvest is the predicted value of the fishery harvest associated with the optimal freshwater inflows. Since many factors have an impact on the optimal solution as discussed previously, the controllable parameters for all six runs of the program, except P_h , are maintained to be the same as much as possible in order to assess the impact of P_h on the optimum.

When P_h is low (e.g., 0.1) all harvest constraints are satisfied automatically (unbinding constraints). When P_h increases to 0.3, only the harvest constraint for blue crab is a binding constraint limiting the allocation of the decision variables (monthly freshwater inflow for major rivers). When P_h increases to 0.5, the number of binding constraints increases to three (red drum, all shrimp, and blue crab), when P_h is 0.6 only sea trout remains to be an unbinding constraint.

Global Optimality

Although the methodology by Bao and Mays (1994) cannot guarantee global optimality, a variety of starting points can help decide the local-global

TABLE 4. Example Results of Optimal Solution of Expected Fish Harvest

Species (1)	Target (1,000 lb) (2)	Expected		Required reliability (5)	Achieved reliability (6)
		Harvest (1,000 lb) (3)	Standard deviation (1,000 lb) (4)		
(a) $P_h = 0.1$, ($S_{cf} = 0.265$ and AL (outerloop) iteration = 5)					
Shellfish	3,034.40	4,066.63	667.15	0.10	0.93
Sea Trout	120.06	322.55	171.24	0.10	0.95
Red Drum	66.75	158.92	55.75	0.10	0.98
All Shrimp	1,935.10	1,920.44	533.91	0.10	0.49
Blue Crab	781.40	487.88	319.47	0.10	0.19
(b) $P_h = 0.3$, ($S_{cf} = 0.193$ and AL (outerloop) iteration = 6)					
Shellfish	3,034.40	4,042.61	663.85	0.30	0.92
Sea Trout	120.06	329.15	177.29	0.30	0.95
Red Drum	66.75	76.74	23.46	0.30	0.62
All Shrimp	1,935.10	1,921.57	534.03	0.30	0.49
Blue Crab	781.40	611.01	315.82	0.30	0.30
(c) $P_h = 0.5$, ($S_{cf} = 0.278$ and AL (outerloop) iteration = 3)					
Shellfish	3,034.40	3,398.77	577.79	0.50	0.73
Sea Trout	120.06	558.06	353.67	0.50	0.98
Red Drum	66.75	70.15	22.67	0.50	0.50
All Shrimp	1,935.10	1,935.10	535.48	0.50	0.50
Blue Crab	781.40	781.40	318.63	0.50	0.50
(d) $P_h = 0.6$, ($S_{cf} = 0.087$ and AL (outerloop) iteration = 5)					
Shellfish	3,034.40	3,171.79	530.19	0.60	0.60
Sea Trout	120.06	578.26	369.14	0.60	0.98
Red Drum	66.75	76.11	24.60	0.60	0.60
All Shrimp	1,935.10	2,078.27	552.51	0.60	0.60
Blue Crab	781.40	865.04	322.78	0.60	0.60

Note: 1 lb = 0.4536 kg.

issue. If all starting points yield approximately the same final solution, then the solution point is more likely to be a global optimal (Lasdon and Waren 1989).

As discussed previously, the values of NDSOQ (the number of calls of $\partial S/\partial Q$ approximating for reduced gradients $\partial F/\partial Q$) affects solution accuracy (Table 1). To consider the tradeoff between computer CPU time and solution accuracy, NDSOQ is selected at either 35 or 10 for model runs at various initial conditions for searching possible global optimum. The results are summarized in Table 5.

The mean of historical annual total flow for both the Lavaca River and the Colorado River is about $1.97 \cdot 10^9$ m³ (1,600,000 acre-ft). The initial monthly flow for each river at a range from $1.233 \cdot 10^6$ m³ to $2.467 \cdot 10^8$ m³ (1,000 to 200,000 acre-ft) is equivalent to the total annual flow of the two rivers at a range from $2.9 \cdot 10^7$ m³ to $5.92 \cdot 10^9$ m³ (24,000 to 4,800,000 acre-ft). To be consistent, the required reliability of harvest chance constraints

TABLE 5. Results of OPTFLOW for Various Initial Monthly Freshwater Inflow Conditions

Case (1)	Initial monthly flow (1,000 acre-ft) (2)	Optimal annual flow (1,000 acre-ft) (3)	Error (percent) (4)	Initial σ (5)	$\Delta\sigma$ (6)	Initial μ (7)	S_c (8)	Total outerloop iteration number (9)	S_{cf} (10)	CPU (s) ^d (11)
(a) NDSOQ = 35										
1	— ^a	1,967.292	—	10.0	10.0	1.0	0.5	4	0.193	444.0
2	1.0 ^b	1,976.998	0.49	10.0	10.0	1.0	0.5	4	0.221	445.2
3	1.0/10.0 ^c	1,971.636	0.22	10.0	10.0	1.0	0.5	4	0.187	444.1
4	10.0	1,985.271	0.91	10.0	10.0	1.0	0.5	4	0.247	445.4
5	50.0	1,963.301	0.20	10.0	10.0	1.0	0.5	4	0.306	444.6
6	100.0	1,971.755	0.23	10.0	10.0	1.0	0.5	4	0.419	444.8
(b) NDSOQ = 10										
1	— ^a	1,890.455	—	10.0	10.0	1.0	0.2	5	0.143	1,328.5
2	1.0 ^b	1,883.123	0.39	10.0	10.0	1.0	0.2	5	0.135	2,657.1
3	10.0 ^c	1,889.128	0.07	10.0	10.0	1.0	0.2	6	0.110	5,309.4
4	50.0	1,877.317	0.69	10.0	10.0	1.0	0.2	5	0.106	2,212.8
5	100.0	1,858.953	1.67	10.0	10.0	1.0	0.2	2	0.179	1,328.2
6	200.0	1,886.476	0.21	10.0	10.0	1.0	0.2	5	0.158	2,213.9

^aThe initial monthly flows are selected near the optimal solution from the previous runs to be used as control case for comparison.

^bSet initial monthly freshwater inflow as $1.2335 \cdot 10^6 \text{ m}^3$ (1,000 acre-ft) for each month for the Lavaca River and the Colorado River to test for the wide variability of initial flow conditions.

^cSet initial monthly freshwater inflow as $1.2335 \cdot 10^6 \text{ m}^3$ (1,000 acre-ft) for each month for the Lavaca River and (10,000 acre-ft) for the Colorado River.

^dAll computations were performed on Cray Y-MP8/864.

Note: 1 acre-ft = $1,233.5 \text{ m}^3$.

(P_h) are fixed at 0.6. The GRG2 parameters are also set at the same values for all six cases. Although the solution accuracy is affected by the large value of NDSOQ (35) and the actual final salinity convergence factor, S_{cf} (equal to the maximum salinity violation, $\max|c_i|$), the relative difference in the annual total flows is consistently less than 1% for all six cases (Fig. 4). The maximum relative error is 1.67% for cases that NDSOQ is equal to 10, which corresponds to the highest final convergence factor of salinity (0.179) and minimum (two) outer loop iterations (Fig. 5). It is easy to see that if the final convergence factor is reduced by some modification of the input data, the maximum relative error will be further reduced.

Considering all twelve cases for various starting points, the difference in the optimal solution of the total annual flow is considered to be acceptable and concludes that the global optimal is likely reached at 1,890,000 acre-ft for a P_h of 0.6.

CONCLUSIONS

The results of numerical application of the new methodology by Bao and Mays (1994) further indicate that the OPTFLOW model is improved over the approaches by Martin (1987) and Tung et al. (1990). Briefly, the new methodology has the capability of incorporating other important factors affecting the salinity in the bay system such as tide, wind, ungauged flow, evaporation, and precipitation; and the capability of presenting the spatial and temporal variability of salinity. The OPTFLOW computer model is a powerful tool for analysis of what-if type scenarios which can be used by a decision maker to analyze various water resources management strategies (or alternatives).

The following conclusions are drawn from the model development and case applications.

1. The approximation scheme for evaluation of the objective function and its reduced gradient with respect to decision variables is reasonable and efficient in reducing the computer execution time. The selection of appropriate NDSOQ (an option to limit the number of approximations of $\partial F/\partial Q$ by $\partial s/\partial Q$) depends on considering the trade-off between solution accuracy and CPU time requirement. For the applications to the Lavaca-Tres Palacios Estuary, NDSOQ is tested for a range from 3 to 500.

2. In general, OPTFLOW converges within five outerloop (augment Lagrangian) iterations, which confirms that the AL method is an efficient algorithm.

3. A high penalty multiplier ($\Delta\sigma$) does not necessarily increase the convergence of the model. The optimal solution of the problem is relatively insensitive to the value of the penalty multiplier. A value of 10 for $\Delta\sigma$ is recommended based on the test runs.

4. The maximum reachable reliability of chance constraints for OPTFLOW is significantly increased as compared to the model by Tung et al. (1990). This is expected because the hydrodynamic transport model has the capability of representing the complex flow circulation, and temporal and spatial variability of salinity. In other words, the hydrodynamic transport model in OPTFLOW reduces uncertainty in the salinity regression equations in the model by Tung et al. (1990).

5. The Tung et al. (1990) model underestimates the minimum annual

optimal flow for low reliability (P_h) values, and overestimates the annual total flow for high (P_h) values. OPTFLOW offers more accurate solutions in these cases.

6. A variety of starting points for OPTFLOW yields the optimum within a 1% difference in total annual freshwater inflows. The local optimal solution is likely to be a global optimum as well.

ACKNOWLEDGMENTS

This research has been funded by the Texas Water Development Board and then by the National Science Foundation under Grant No. BCS-9104406. Special thanks goes to the reviewers for their very helpful suggestions and to George Ward of the Center for Research in Water Resources at the University of Texas at Austin, and to Junji Matsumoto and Gary Powell of the Texas Water Development Board.

APPENDIX. REFERENCES

- Bao, Y. X. (1992). "Methodology for determining the optimal freshwater inflows into bays and estuaries," PhD dissertation, Dept. of Civil Engineering, Univ. of Texas at Austin, Austin, Tex.
- Bao, Y. X., Tung, Y. K., Mays, L. W., and Ward, W. H. Jr. (1989). "Analysis of the effect of freshwater inflows on estuary fishery resources," *Tech. Memo. 89-2*, Center for Research in Water Resources, Univ. of Texas at Austin, Austin, Tex.
- Bao, Y. X., and Mays, L. W. (1994). "New methodology for optimization of freshwater inflows to estuaries." *J. Water Resour. Plng. and Mgmt.*, ASCE, 120(2), 199–217.
- Fletcher, R. (1975). "An ideal penalty function for constrained optimization." *J. Inst. of Math. and Its Applications*, 15, 319–342.
- Lasdon, L. S., and Waren, A. D. (1989). *GRG2 user's guide*. Dept. of General Business, Univ. of Texas at Austin, Austin, Tex.
- "Lavaca-Tres Palacios estuary: a study of the influence of freshwater flows." (1980). *Rep. LP-106*, Texas Department of Water Resources, Austin, Tex.
- Martin, Q. W. (1987). "Estimating freshwater inflow needs for Texas estuaries by mathematical programming." *Water Resour. Res.*, 23(2), 230–238.
- "Mathematical simulation capabilities in water resource systems analysis." (1979). *Rep. LP-16*, Texas Department of Water Resources, Austin, Tex.
- Tung, Y. K., Bao, Y. X., Mays, L. W., and Ward, W. H. (1990). "Optimization of freshwater inflow to estuaries." *J. Water Resour. Plng. and Mgmt.* 116(4), 567–584.